

Exploring twist-3 chiral even generalized parton distributions of light sea quarks in the proton using the light front model

Parashmani Thakuria¹^{*}, Madhurjya Lalung²[†] and Jayanta Kumar Sarma¹[‡]

¹*Department of Physics, School of Sciences, Tezpur University, Tezpur, India, Pin-784028 and*

²*Department of Physics, Nagaon University, Nagaon, India*

(Dated: November 5, 2024)

We develop a light-front model of the proton to investigate the twist-3 chiral-even generalized parton distributions (GPDs) of light sea quarks. In this model, the sea quarks are treated as spin- $\frac{1}{2}$ active partons, while the remaining proton constituents are modeled as spin-1 spectators. The momentum wave function, predicted by the soft-wall AdS/QCD, is fitted to the unpolarized parton distribution functions (PDFs) from the CETQ global analysis. Using this fitted distribution, we determine the unknown model parameters. We calculate the twist-3 GPDs and analyze their dependence on the transverse momentum transfer, Δ_T^2 , and the longitudinal momentum fraction, x . Additionally, we explore the Mellin moments and the twist-3 chiral-even PDF, $g_T(x)$, within this theoretical framework.

I. INTRODUCTION

It is an extremely challenging task to understand the internal three-dimensional structure of a proton in terms of its constituent partons (quarks, gluons) [1–6]. With the help of parton distribution functions (PDFs), the one-dimensional function of the longitudinal momentum fraction and extensive study of the internal structures are carried out. PDFs are forward, diagonal matrix elements that provide a probabilistic interpretation for the operator chosen. Unlike PDFs, GPDs also depend on the squared momentum transfer (t) and the longitudinal momentum transfer (or skewness ξ). GPDs are off-forward matrix elements of non-local operators and can be accessed experimentally through processes like deeply virtual Compton scattering (DVCS) [7–10] or deeply virtual meson production (DVMP) [11–14]. Experimental data for these processes have been collected by collaborations like H1 [15, 16], ZEUS [15, 17], and fixed-target experiments at HERMES [18, 19], COMPASS [20], and JLab [21, 22]. Considerable progress on the theoretical side has also been observed. Because of the perturbative nature of GPDs, they can't be directly calculated from the first principle of QCD. Although ongoing lattice calculations will provide more insides. Therefore, model calculations are carried out, such as the MIT bag model [23], the light-front constituent quark model [2, 24–26], the NJL model [27], the color glass condensate model [28], the chiral quark-soliton model [29, 30], the Bethe-Salpeter approach [31, 32] and the meson cloud model [33, 34].

Parton distribution functions (PDFs) are categorized by their twist, which refers to their order in a $1/Q$ expansion, where Q denotes the hard scale associated with the underlying physical process. While most research on generalized parton distributions (GPDs) has focused

on leading-twist contributions, higher-twist GPDs, particularly those of twist-3, remain comparatively under-explored. Nevertheless, twist-3 GPDs provide valuable insights into the partonic structure of hadrons. Notably, there is a connection between quark orbital angular momentum within the nucleon and twist-3 GPDs [6, 35, 36]. The amplitude of deeply virtual Compton scattering (DVCS) at twist-3 can be expressed in terms of twist-3 GPDs through the Compton form factor [37]. Some studies suggest that twist-3 GPDs can also offer insights into the average transverse color Lorentz force acting on quarks [38],[39]. However, experimentally determining higher-twist distributions is challenging, as they are difficult to disentangle from leading-twist contributions. Moreover, higher-twist contributions are typically smaller, owing to suppression factors. The twist-3 GPDs have been investigated in the quark target model [40–42] and scalar diquark model [42] for the nucleon. The twist-4 proton GPDs were studied within the light-front quark-diquark model (LFQDM) recently [43], and the chiral-even twist-3 GPDs of the proton have also been investigated by the Lattice QCD [44]. The calculations of the twist-3 GPDs chiral-even GPDs of the protons have been carried out in the basis light-front quantization (BLFQ collaboration) [45] with the overlap representations of light-front wave functions.

In this work we have developed a light-front spectator model for proton to study the light sea quarks (\bar{u}, \bar{d}), which are considered as spin-1/2, and the remaining spin-1 particle is considered as a spectator. We have used the momentum wave function predicted by the soft-wall AdS/QCD. The model parameters are determined by fitted unpolarized sea quarks PDF from CTEQ global analysis at scale $Q_0 = 2 \text{ GeV}$. We have investigated the behaviors of twist-3 GPDs at different energy scales and x -values. The higher-order Mellin moments of GPDs are also investigated, and we have given the values of Mellin moments in table [2-3], which are calculated from the model under study. In the forward limit and chiral even case, we have only one PDF, g_T , and we have investigated the PDF at different values of $-t'$.

* parasht@tezu.ernet.in

† mlalung2016@gmail.com

‡ jks@tezu.ernet.in

In Section I, we present an introduction to the subject matter. Section II provides a detailed calculation of the overlap representation for the twist-3 generalized parton distributions (GPDs). In Section III, we discuss the light-front model used in this study. This is followed by a fit of the unpolarized parton distribution functions (PDFs), calculated from the model, to the CT18NNLO data in order to evaluate the model parameters. In Part III B of Section III, we derive the expression for the twist-3 GPDs. Finally, the results and discussion are presented in Section IV.

II. CHIRAL EVEN GPDS IN OVERLAP REPRESENTATION

The Generalized Parton Distributions (GPDs) are defined as non-forward matrix elements of the quark-quark correlator function. In light cone coordinate, the quark-quark correlator [46] is commonly written as,

$$F_{[\Lambda', \Lambda]}^\Gamma(x, \xi, t) = \frac{1}{2} \int \frac{dz^-}{2\pi} e^{ix\bar{P}^+ z^-} \langle p', \Lambda' | \bar{\psi}(-\frac{z}{2}) \Gamma \mathcal{W}\left(\frac{-z}{2}, \frac{z}{2}\right) \psi(+\frac{z}{2}) | p, \Lambda \rangle \Big|_{z^+=0, z_T=0} \quad (1)$$

$$F_{\Lambda\Lambda'}^{\gamma^j} = \left[\frac{\Delta^j}{2P^+} (E_{2T} + 2\tilde{H}_{2T}) + \frac{i\Lambda\epsilon^{jk}\Delta^k}{2P^+} (\tilde{E}_{2T} - \xi E_{2T}) \right] \delta_{\Lambda\Lambda'} + \left[\frac{-M(\Lambda\delta_{j1} + i\delta_{j2})}{P^+} H_{2T} - \frac{(\Lambda\Delta^1 + i\Delta^2)\Delta^j}{2MP^+} \tilde{H}_{2T} \right] \delta_{\Lambda-\Lambda'} \quad (3)$$

$$F_{\Lambda\Lambda'}^{\gamma^j\gamma_5} = \left[\frac{i\epsilon^{jk}\Delta^k}{2P^+} (E'_{2T} + 2\tilde{H}'_{2T}) - \frac{\Lambda\Delta^j}{2P^+} (\tilde{E}'_{2T} - \xi E'_{2T}) \right] \delta_{\Lambda\Lambda'} + \left[\frac{M(\delta_{j1} + i\Lambda\delta_{j2})}{P^+} H'_{2T} - \frac{i\epsilon^{jk}(\Lambda\Delta^1 + i\Delta^2)\Delta^k}{2MP^+} \tilde{H}'_{2T} \right] \delta_{\Lambda-\Lambda'} \quad (4)$$

The antisymmetric tensor is defined by $\epsilon^{ij} = 1 = -\epsilon^{ji}$ and $P = (p + p')/2$ is the average proton momentum, $\Delta = p - p'$ is the momentum transfer with $t = \Delta^2 = -\Delta_T^2$ and $\xi = -\Delta^+/2P^+$ is the skewness parameter. We denote ‘ \pm ’ as the proton helicity. Since $j = 1, 2$, the parameterization given in equations 3 and 4 can be reduced according to possible helicity combinations. These combinations are listed in Appendix A from equations A1-A8. Using these equations, we can derive the explicit formula of the GPDs in overlap representations, which are given below,

$$-\frac{2i\Delta^1\Delta^2}{MP^+} \tilde{H}_{2T} = (F_{[+-]}^{\gamma^1} + F_{[-+]}^{\gamma^1}) + i(F_{[+-]}^{\gamma^2} - F_{[-+]}^{\gamma^2}) \quad (5)$$

Where Γ is the Dirac bilinear and Λ, Λ' are the target initial and final state helicities. \mathcal{W} is the Wilson line, which plays a critical role in ensuring gauge invariance of the nonlocal operator product. It is a path-ordered exponential that connects the quark fields along the light cone, compensating for gauge transformations along the path and maintaining the physical observability of the GPDs. The general definition of \mathcal{W} is,

$$\mathcal{W}\left(\frac{-z}{2}, \frac{z}{2}\right) = P \exp\left(ig \int_a^b dx^- A^+(x^- n_-)\right) \quad (2)$$

Here P denotes the path ordering from a to b . We have to consider the light-cone gauge where $A^+ = 0$. So the value of \mathcal{W} is 1, which also makes it $SU(3)$ color gauge invariant.

The key Dirac bilinears relevant to twist-3 chiral-even generalized parton distributions are given by $\Gamma = \gamma^j, \gamma^j\gamma_5$. Consequently, the parameterization of Equation 1, as provided in [46, 47], for these bilinears is expressed as follows:

$$-\frac{4M}{P^+} H_{2T} - \frac{\Delta_T^2}{MP^+} \tilde{H}_{2T} = (F_{[+-]}^{\gamma^1} - F_{[-+]}^{\gamma^1}) - i(F_{[+-]}^{\gamma^2} + F_{[-+]}^{\gamma^2}) \quad (6)$$

$$\frac{\Delta^1 + i\Delta^2}{P^+} (\tilde{E}_{2T} - \xi E_{2T}) = (F_{[+-]}^{\gamma^1} - F_{[-+]}^{\gamma^1}) + i(F_{[+-]}^{\gamma^2} - F_{[-+]}^{\gamma^2}) \quad (7)$$

$$\frac{\Delta^1 + i\Delta^2}{P^+} (E_{2T} + 2\tilde{H}_{2T}) = (F_{[+-]}^{\gamma^1} + F_{[-+]}^{\gamma^1}) + i(F_{[+-]}^{\gamma^2} + F_{[-+]}^{\gamma^2}) \quad (8)$$

$$\frac{2i\Delta^1\Delta^2}{MP^+}\tilde{H}'_{2T} = (F_{[+-]}^{\gamma^1\gamma_5} - F_{[-+]}^{\gamma^1\gamma_5}) - i(F_{[+-]}^{\gamma^2\gamma_5} + F_{[-+]}^{\gamma^2\gamma_5}) \quad (9)$$

$$\frac{\Delta^1 + i\Delta^2}{P^+}(E'_{2T} + 2\tilde{H}'_{2T}) = (F_{[++]}^{\gamma^1\gamma_5} + F_{[--]}^{\gamma^1\gamma_5}) + i(F_{[++]}^{\gamma^2\gamma_5} + F_{[--]}^{\gamma^2\gamma_5}) \quad (10)$$

$$\frac{4M}{P^+}H'_{2T} + \frac{\Delta^1 + i\Delta^2}{MP^+}\tilde{H}'_{2T} = (F_{[+-]}^{\gamma^1\gamma_5} + F_{[-+]}^{\gamma^1\gamma_5}) + i(F_{[+-]}^{\gamma^2\gamma_5} - F_{[-+]}^{\gamma^2\gamma_5}) \quad (11)$$

$$-\left(\frac{\Delta^1 + i\Delta^2}{P^+}\right)(\tilde{E}'_{2T} - \xi E'_{2T}) = (F_{[++]}^{\gamma^1\gamma_5} - F_{[--]}^{\gamma^1\gamma_5}) + i(F_{[++]}^{\gamma^2\gamma_5} - F_{[--]}^{\gamma^2\gamma_5}) \quad (12)$$

III. LIGHT FRONT MODEL FOR THE PROTON

In this section to investigate the sea quarks (\bar{u}, \bar{d}) chiral even generalized parton distribution in proton, we have formulated a light cone spectator model following the steps described in [48]. To generate the sea quark degree of freedom, we have considered the Fock state $|qqq\bar{q}q\rangle$. The proton is then reduced to a two-particle system. Sea quark is considered an active parton having spin-1/2, and all the other valance quarks and gluons are considered spin-1 spectators.

Throughout the calculations, we have followed the convention $x^\pm = x^0 \pm x^3$. We have considered the frame of reference where the transverse momentum of a proton is zero such that $P = (P^+, \frac{M^2}{P^+}, 0_T)$. The two particle Fock state is $|\lambda_q, \lambda_X, xP^+, \mathbf{k}_T\rangle$, with λ_q and λ_X being the helicities of the sea quark and the spectator. We have used the notation ‘ \pm ’ for quark and ‘ \uparrow (\downarrow)’ for spectator.

The two particle Fock-state expansion can be written as [48] with proton helicity $J_Z = \pm \frac{1}{2}$ as

$$\Psi_{\text{Two particle}}^\pm = \int \frac{dx d^2\mathbf{k}_T}{16\pi^3 \sqrt{x(1-x)}} \times \left[\psi_+^\pm(x, \vec{k}_T, \uparrow)|+, \uparrow; xP^+, \vec{k}_T\rangle + \psi_+^\pm(x, \vec{k}_T, \downarrow)|+, \downarrow; xP^+, \vec{k}_T\rangle + \psi_-^\pm(x, \vec{k}_T, \uparrow)|-, \uparrow; xP^+, \vec{k}_T\rangle + \psi_-^\pm(x, \vec{k}_T, \downarrow)|-, \downarrow; xP^+, \vec{k}_T\rangle \right] \quad (13)$$

The two particle LFWFs of proton with $J_Z = +1/2$ is,

$$\begin{aligned} \psi_+^+(x, \mathbf{k}_T, \uparrow) &= -\sqrt{2} \frac{-k_1 + ik_2}{x(1-x)} \varphi(x, \mathbf{k}_T) \\ \psi_+^+(x, \mathbf{k}_T, \downarrow) &= -\sqrt{2} \frac{k_1 + ik_2}{1-x} \varphi(x, \mathbf{k}_T) \\ \psi_-^+(x, \mathbf{k}_T, \uparrow) &= -\sqrt{2} \left(M - \frac{M_X}{1-x} \right) \varphi(x, \mathbf{k}_T) \\ \psi_-^+(x, \mathbf{k}_T, \downarrow) &= 0 \end{aligned} \quad (14)$$

and for $J_z = -\frac{1}{2}$ we have the following LFWFs,

$$\begin{aligned} \psi_+^-(x, \mathbf{k}_T, \uparrow) &= 0 \\ \psi_+^-(x, \mathbf{k}_T, \downarrow) &= -\sqrt{2} \left(M - \frac{M_X}{1-x} \right) \varphi(x, \mathbf{k}_T) \\ \psi_-^-(x, \mathbf{k}_T, \uparrow) &= -\sqrt{2} \frac{-k_1 + ik_2}{1-x} \varphi(x, \mathbf{k}_T) \\ \psi_-^-(x, \mathbf{k}_T, \downarrow) &= -\sqrt{2} \frac{k_1 + ik_2}{x(1-x)} \varphi(x, \mathbf{k}_T) \end{aligned} \quad (15)$$

M and M_X represent the mass of proton and spectator. Here $\varphi(x, \mathbf{k}_T)$ is the modified soft-wall AdS/QCD momentum wave function. We have used the wave function that was given in [49] and it has the expression,

$$\begin{aligned} \varphi(x, \mathbf{k}_T) &= \sqrt{A} \frac{4\pi}{\kappa} \sqrt{\frac{\log[\frac{1}{1-x}]}{x}} x^\alpha (1-x)^{3+\beta} \\ &\quad \text{Exp} \left[-\frac{\log[\frac{1}{1-x}]}{2\kappa^2 x(1-x)} \mathbf{k}_T^2 \right] \end{aligned} \quad (16)$$

The AdS scale parameter is $\kappa = 0.4 \text{ GeV}$ [50], and A , α , and β are model-dependent parameters. They are fixed by fitting unpolarized sea quark PDF with CT18NNLO data set at energy scale 2 GeV. We have considered $M_X = 0.946 \text{ GeV}$. The values of the model parameters for the up- and down-sea quarks are given in I.

A. Model parameter fitting

The non-perturbative structures of hadron are studied using parton distributions. Physically, it gives the probability of finding a parton with longitudinal momentum fraction ‘ x ’. The unpolarized sea quark PDF in our model is expressed as,

$$\begin{aligned}
f_1(x) &= \int \frac{d^2 \mathbf{k}_T}{16\pi^3} [|\psi_+^+(x, \mathbf{k}_T, \uparrow)|^2 + |\psi_-^+(x, \mathbf{k}_T, \uparrow)|^2 \\
&\quad + |\psi_+^+(x, \mathbf{k}_T, \downarrow)|^2 + |\psi_-^+(x, \mathbf{k}_T, \downarrow)|^2] \\
&= \int \frac{d^2 \mathbf{k}_T}{16\pi^3} [|\psi_-^-(x, \mathbf{k}_T, \uparrow)|^2 + |\psi_+^-(x, \mathbf{k}_T, \uparrow)|^2 \\
&\quad + |\psi_-^-(x, \mathbf{k}_T, \downarrow)|^2 + |\psi_+^-(x, \mathbf{k}_T, \downarrow)|^2] \\
&= 2Ax^{2\alpha}(1-x)^{7+2\beta} \left[\frac{\kappa^2(1+x^2)}{x(1-x)\log(\frac{1}{1-x})} \right. \\
&\quad \left. + \left(M - \frac{M_X}{1-x} \right)^2 \right] \quad (17)
\end{aligned}$$

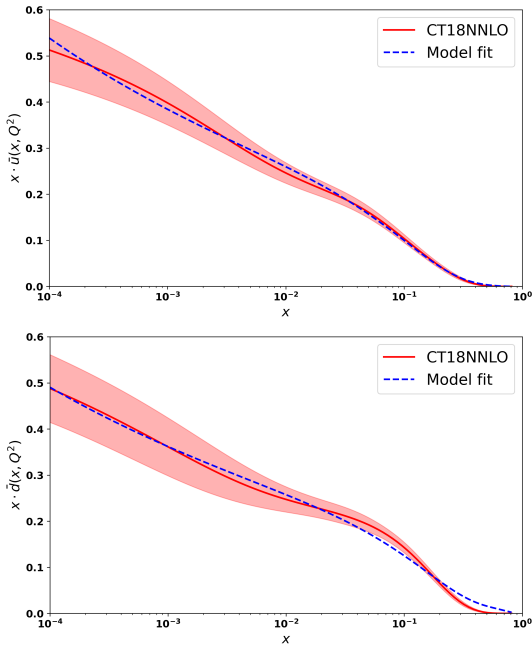


FIG. 1: Sea quark unpolarized PDFs in the proton; $x\bar{u}$ is in the top figure and $x\bar{d}$ is in the bottom figure.

	A	α	β
\bar{u}	0.4462 ± 0.0096	0.4279 ± 0.0016	0.0742 ± 0.0870
\bar{d}	0.4622 ± 0.0076	0.4349 ± 0.0010	-0.9817 ± 0.0351

TABLE I: Fitted parameters for \bar{u} and \bar{d} quark distributions.

$$\begin{aligned}
\frac{\Delta^1 + i\Delta^2}{P^+} E_{2T}' = - \int \frac{d^2 \mathbf{k}_T}{16\pi^3} \frac{2m}{x} \left(\frac{\Delta^1 + i\Delta^2}{\Delta^1 \Delta^2} \right) &\left\{ \psi_+^{\dagger}(x, \mathbf{k}_T'', \uparrow) \psi_-^-(x, \mathbf{k}_T', \uparrow) + \psi_+^{\dagger}(x, \mathbf{k}_T'', \downarrow) \right. \\
&\left. \psi_-^-(x, \mathbf{k}_T', \downarrow) - \psi_-^{\dagger}(x, \mathbf{k}_T'', \uparrow) \psi_+^+(x, \mathbf{k}_T', \uparrow) - \psi_-^{\dagger}(x, \mathbf{k}_T'', \downarrow) \psi_+^+(x, \mathbf{k}_T', \downarrow) \right\} \quad (20)
\end{aligned}$$

We have followed the procedure provided by [49] to determine the model parameters. In our model, the parameters are α, β and A . The parameter A is a free parameter, and it describes the amplitude of sea quarks PDF in the $x = 0$ region. The α parameter controls the low x value, and the β parameter controls the high x value. In fig 1, the top figure is for $x\bar{u}$ and the bottom figure is for $x\bar{d}$. Since the model relies on only three parameters, it has a notable advantage.

B. Chiral even GPDs at zero skewness

The quark-quark correlator, as presented in [43], is expressed in the overlap representation at $\xi = 0$ as,

$$\begin{aligned}
F_{[\Lambda'\Lambda]}^\Gamma(x, 0, t) &= \int \frac{d^2 \mathbf{k}_T}{16\pi^3} \sum_{\lambda_{q_i}} \sum_{\lambda_{q_f}} \psi_{\lambda_{q_f}}^{\Lambda'\dagger}(x, \mathbf{k}_T'', \lambda_X) \psi_{\lambda_{q_i}}^\Lambda(x, \mathbf{k}_T', \lambda_X) \\
&\quad \frac{u_{\lambda_{q_f}}^\dagger(xP^+, \mathbf{k}_T + \frac{\Delta_T}{2}) \gamma^0 \Gamma u_{\lambda_{q_i}}(xP^+, \mathbf{k}_T - \frac{\Delta_T}{2})}{2xP^+} \quad (18)
\end{aligned}$$

In this context, λ_{q_i} and λ_{q_f} denote the initial and final helicities of the sea quark, respectively. In the overlap representation, Δ is treated as a two-dimensional complex vector, defined by $\Delta = \Delta^1 + i\Delta^2$. The expression

$$u_{\lambda_{q_f}}^\dagger \left(xP^+, \mathbf{k}_T + \frac{\Delta_T}{2} \right) \gamma^0 \Gamma u_{\lambda_{q_i}} \left(xP^+, \mathbf{k}_T - \frac{\Delta_T}{2} \right)$$

represents the spinor product associated with higher-twist Dirac matrices. The Dirac matrices within the light-cone formalism are comprehensively detailed in [51, 52]. The initial and final transverse momenta of the struck sea quark are,

$$\mathbf{k}_T'' = \mathbf{k}_T + (1-x) \frac{\Delta_T}{2}, \quad \mathbf{k}_T' = \mathbf{k}_T - (1-x) \frac{\Delta_T}{2} \quad (19)$$

At zero skewness ($\xi = 0$), only four chiral GPDs remain, as shown using the symmetry properties of GPDs in [45]. Therefore, the chiral-even GPDs of sea quarks can be derived from equations 5-12,

$$\begin{aligned}
& \frac{\Delta^1 + i\Delta^2}{P^+} \tilde{E}_{2T} \\
&= \int \frac{d^2\mathbf{k}_T}{16\pi^3} \frac{1}{2x^2M^2} \left\{ \left(x^2M^2 + m^2 - \mathbf{k}_T^2 + \frac{\Delta_T^2}{4} \right) (\psi_+^{+\dagger}(x, \mathbf{k}_T'', \uparrow) \psi_-^+(x, \mathbf{k}'_T, \uparrow) + \psi_-^{+\dagger}(x, \mathbf{k}_T'', \uparrow) \psi_+^+(x, \mathbf{k}'_T, \uparrow)) \right. \\
&\quad - \psi_+^{-\dagger}(x, \mathbf{k}_T'', \downarrow) \psi_-^-(x, \mathbf{k}'_T, \downarrow) - \psi_-^{-\dagger}(x, \mathbf{k}_T'', \downarrow) \psi_+^-(x, \mathbf{k}'_T, \downarrow) + \left(\frac{\Delta_T^2}{4} - x^2M^2 - m^2 - \mathbf{k}_T^2 \right) (\psi_+^{+\dagger}(x, \mathbf{k}_T'', \uparrow) \\
&\quad \left. \psi_-^+(x, \mathbf{k}'_T, \uparrow) + \psi_-^{+\dagger}(x, \mathbf{k}_T'', \uparrow) \psi_+^+(x, \mathbf{k}'_T, \uparrow) - \psi_+^{-\dagger}(x, \mathbf{k}_T'', \downarrow) \psi_-^-(x, \mathbf{k}'_T, \downarrow) - \psi_-^{-\dagger}(x, \mathbf{k}_T'', \downarrow) \psi_+^-(x, \mathbf{k}'_T, \downarrow) \right\} \quad (21)
\end{aligned}$$

$$\begin{aligned}
\frac{2i\Delta^1\Delta_2}{MP^+} \tilde{H}'_{2T} &= \int \frac{d^2\mathbf{k}_T}{16\pi^3} \frac{2m}{xM} \left\{ \psi_+^{+\dagger}(x, \mathbf{k}_T'', \uparrow) \psi_-^-(x, \mathbf{k}'_T, \uparrow) + \psi_+^{+\dagger}(x, \mathbf{k}_T'', \downarrow) \psi_-^-(x, \mathbf{k}'_T, \downarrow) - \psi_-^{-\dagger}(x, \mathbf{k}_T'', \uparrow) \psi_+^+(x, \mathbf{k}'_T, \uparrow) \right. \\
&\quad \left. - \psi_-^{-\dagger}(x, \mathbf{k}_T'', \downarrow) \psi_+^+(x, \mathbf{k}'_T, \downarrow) \right\} \quad (22)
\end{aligned}$$

$$\begin{aligned}
\frac{4M}{P^+} H'_{2T} &= \int \frac{d^2\mathbf{k}_T}{16\pi^3} \frac{2m}{xM} \left\{ \psi_-^{-\dagger}(x, \mathbf{k}_T'', \uparrow) \psi_+^+(x, \mathbf{k}'_T, \uparrow) + \psi_-^{-\dagger}(x, \mathbf{k}_T'', \downarrow) \psi_+^+(x, \mathbf{k}'_T, \downarrow) - \frac{\Delta_T^2}{2\Delta^1\Delta^2} \left(\psi_+^{+\dagger}(x, \mathbf{k}_T'', \uparrow) \psi_-^-(x, \mathbf{k}'_T, \uparrow) \right. \right. \\
&\quad \left. \left. + \psi_+^{+\dagger}(x, \mathbf{k}_T'', \downarrow) \psi_-^-(x, \mathbf{k}'_T, \downarrow) - \psi_-^{-\dagger}(x, \mathbf{k}_T'', \uparrow) \psi_+^+(x, \mathbf{k}'_T, \uparrow) - \psi_-^{-\dagger}(x, \mathbf{k}_T'', \downarrow) \psi_+^+(x, \mathbf{k}'_T, \downarrow) \right) \right\} \quad (23)
\end{aligned}$$

The light-front wave functions from equations (14) and (15) are applied to the generalized parton distributions (GPDs) in equations (20), (21), (22), and (23). Subsequently, the integration over the transverse momentum \mathbf{k}_T is carried out to derive the analytical expressions of the GPDs. The limit of the \mathbf{k}_T integration is from 0 to ∞ . In this calculations we have some used standard Gaussian integrals. These integrals are listed in appendix B.

IV. RESULT AND DISCUSSION

In this section we have presented the analytical results of twist-3 chiral even GPDs of light sea quarks in the proton at zero skewness in the light front spectator framework. We have also calculated the numerical results of Mellin moments as well as twist-3 on the gravitational form factor $B(t)$. The twist-3 PDF (g_T) is investigated, and we have also examined the Burkhardt-Cottingham sum rule [53] for \bar{u} and \bar{d} .

A. Twist-3 chiral even GPDs

We have analytically solved GPDs within our model using the overlap representation presented in equations (26)-(29). Since $\xi = 0$, we have investigated the GPDs as a function of x and $-t$. In our calculation we have found that \tilde{E}_{2T} , \tilde{H}'_{2T} , E'_{2T} and H'_{2T} are non-zero and all other chiral even GPDs are zero, which is consistent with [45].

The only γ^i structure that remains at zero skewness is \tilde{E}_{2T} . In Figure 2, we present plots of $x^2\tilde{E}_{2T}$ as functions of x and Δ_T^2 for both sea quark flavors. A symmetry is observed for the \bar{u} and \bar{d} flavors, which arises due to the longitudinal polarization of the proton. The 3D plot for \bar{u} shows a peak at $x = 0.14$, while for \bar{d} the peak occurs at $x = 0.23$. This difference in peak positions is attributed to the presence of the quark mass term in the GPDs expression. Both plots exhibit a Gaussian-like nature. The structures \tilde{H}'_{2T} , E'_{2T} , and H'_{2T} , which correspond to the $\gamma^i\gamma_5$ components, also survive at zero skewness. Figure 3 displays the 3D plots of these structures against Δ_T^2 and x . The function $x^2E'_{2T}$ demonstrates the same Gaussian characteristics as $x^2\tilde{E}_{2T}$. For \bar{u} , the peak is located

at $x = 0.123$, while for \bar{d} , it is found at $x = 0.2$. Notably, \tilde{H}'_{2T} and H'_{2T} exhibit similar but negative distributions. The quantity $x^2 \tilde{H}'_{2T}$ decreases more sharply than $x^2 H'_{2T}$ in the energy range $\Delta_T^2 = (0.1 - 0.2) \text{ GeV}^2$. Specifically, $x^2 \tilde{H}'_{2T}$ peaks at $x = 0.18$ for \bar{d} and $x = 0.123$ for \bar{u} . For $x^2 H'_{2T}$, the peaks occur at $x = 0.18$ for \bar{d} and $x = 0.12$ for \bar{u} .

The chiral-even generalized parton distributions (GPDs) $x^2 \tilde{E}'_{2T}$, $x^2 \tilde{H}'_{2T}$, $x^2 E'_{2T}$, and $x^2 H'_{2T}$ are plotted at fixed values of transverse momentum transfer Δ_T^2 and longitudinal momentum fraction x to enhance our understanding. In Figure 6, we present the GPDs at fixed Δ_T^2 values of 0.25 GeV^2 , 0.50 GeV^2 , and 0.75 GeV^2 , where the left column figures correspond to \bar{u} and the right column figures correspond to \bar{d} .

We observe that $x^2 \tilde{E}'_{2T}$ and $x^2 E'_{2T}$ increase as the longitudinal momentum x increases, peaking between

$x = 0.1$ and 0.25 before beginning to decrease. The highest maxima occur at lower values of Δ_T^2 , while for larger values of Δ_T^2 , the GPDs become negligible. A similar pattern is observed for $x^2 \tilde{H}'_{2T}$ and $x^2 H'_{2T}$; however, they begin to decrease and reach a minimum in the range of $x = 0.1$ to 0.2 for both sea quarks \bar{u} and \bar{d} , before increasing again. For larger values of Δ_T^2 , the GPDs approach zero.

We also plot the GPDs at fixed values of $x = 0.1, 0.3,$ and 0.5 while varying Δ_T^2 from 0 to 1 GeV^2 . Key observations indicate that as Δ_T^2 increases, the GPDs ($x^2 \tilde{E}'_{2T}$ and $x^2 E'_{2T}$) fall sharply and asymptotically approach zero. With increased fixed values of x , the GPD values become negligible. Similar trends are noted for the other GPDs, which also start increasing sharply and then asymptotically approach zero.

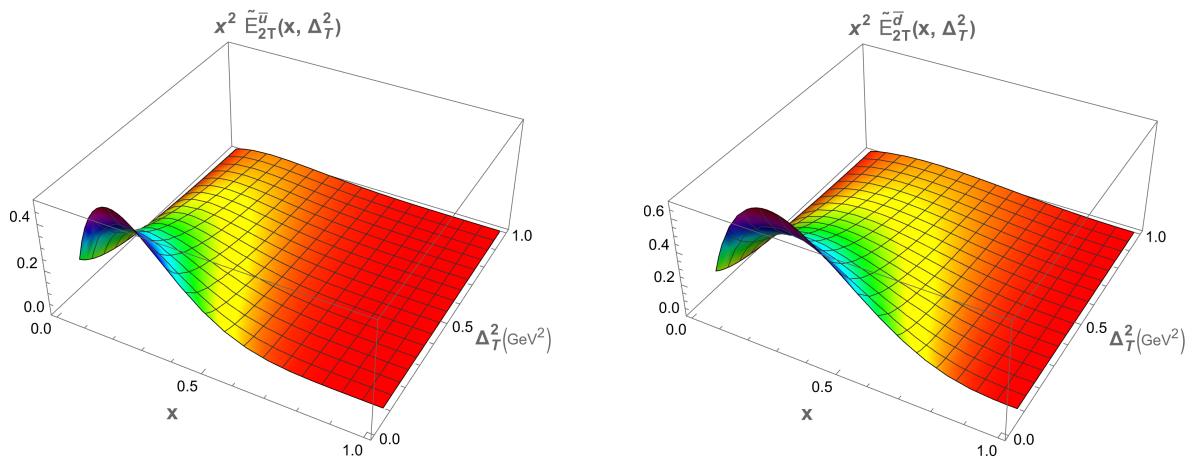


FIG. 2: The twist-3 chiral even light sea quark GPDs in the proton for the Dirac bilinears $\Gamma = \gamma^i$ are shown. The left plot corresponds to the distribution for \bar{u} , while the right plot corresponds to the distribution for \bar{d} .

B. Mellin moments of twist-3 GPDs

Mellin moments are powerful tools that relate the internal structure of hadrons with measurable quantities like form factors and parton distribution functions (PDFs). The Mellin moments of GPDs can be linked to generalized form factors (GFFs). Mathematically, they are defined as,

$$M_n(t) = \int_{-1}^1 dx x^n X(x, \xi, t) \quad (24)$$

We have numerically evaluated the Mellin moments using Eq. 24 at zero skewness. The generalized parton distributions (GPDs) under investigation are denoted as $X(x, t)$. The zeroth Mellin moment ($n = 0$) corresponds to the form factor associated with the total momentum carried by the quarks. Higher Mellin moments ($n \geq 1$)

can give access to various components of the angular momentum and the distribution of forces inside the hadron. In Table II, the calculations are presented for the \bar{u} distribution for $n = 0, 1,$ and 2 . Similarly, Table III shows the results for the \bar{d} distribution for $n = 0, 1,$ and 2 . The Mellin moment calculation can be tested in future lattice calculations and high-precision experiments to validate the model.

	$n = 0$	$n = 1$	$n = 2$
\tilde{E}'_{2T}	3.03478	0.548378	0.119956
\tilde{H}'_{2T}	-0.00379745	-0.000647706	-0.000130139
H'_{2T}	-0.0000506056	-8.63147×10^{-6}	-1.73426×10^{-6}
E'_{2T}	0.00759489	0.00129541	0.000260278

TABLE II: Model calculations of Mellin moments of \bar{u} quark in proton.

To study the gravitational form factors we have adopted a different parameterization given in [54],

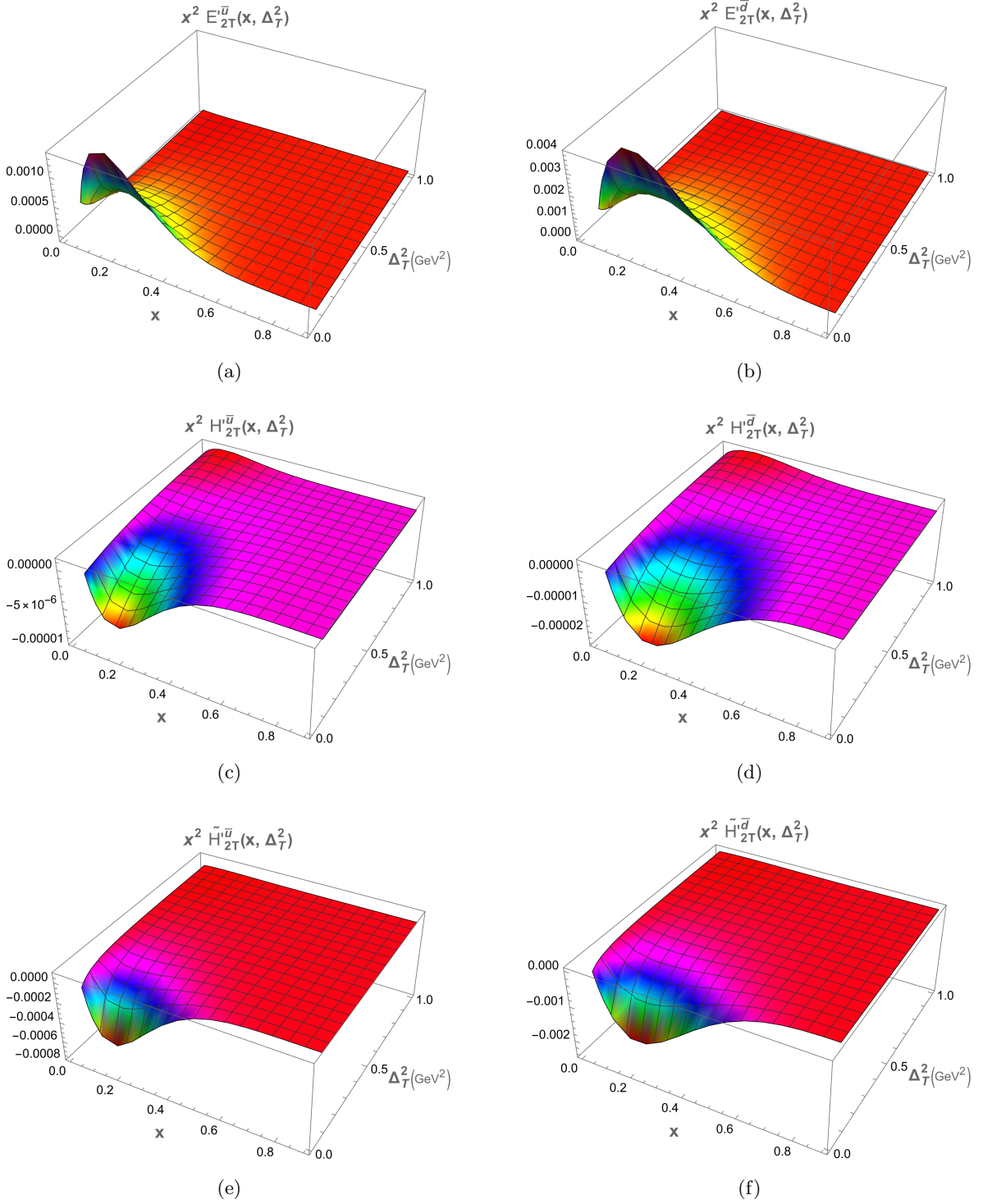


FIG. 3: The twist-3 chiral even light sea quark GPDs in the proton for the Dirac bilinears $\Gamma = \gamma^i \gamma_5$, are plotted. The left column of the plots corresponds to the distributions for \bar{u} , while the right column corresponds to \bar{d} .

$$F_{q,\gamma^\perp} = \frac{\bar{\Delta}^\perp}{M} G_{q,1}(x, \xi, -t) + \bar{\Delta}^\perp \not{n} G_{q,2}(x, \xi, -t) + \frac{i\sigma^{\perp\rho} \Delta_\rho}{2M} G_{q,3}(x, \xi, -t) + M i\sigma^{\perp\rho} n_\rho G_{q,4}(x, \xi, -t) \quad (25)$$

By comparing them with the ones in equation 3, we have the following relations between the GPDs [54],

	$n = 0$	$n = 1$	$n = 2$
\bar{E}_{2T}	4.9224	1.03145	0.277907
\bar{H}'_{2T}	-0.0127497	-0.00242491	-0.000568928
H'_{2T}	-0.000169905	-0.0000323149	-7.58166×10^{-6}
E'_{2T}	0.0254994	0.00484982	0.00113786

TABLE III: Model calculations of Mellin moments of \bar{d} quark in proton.

$$E_{2T}(x, \xi, -t) = 2G_{q,2}(x, \xi, -t) \quad (26)$$

$$H_{2T}(x, \xi, -t) = G_{q,4}(x, \xi, -t) \quad (27)$$

$$\tilde{E}_{2T}(x, \xi, -t) = 2\xi G_{q,2}(x, \xi, -t) - G_{q,3}(x, \xi, -t) \quad (28)$$

$$\tilde{H}_{2T}(x, \xi, -t) = G_{q,1}(x, \xi, -t) \quad (29)$$

However, at zero skewness ($\xi = 0$), only one of the above GPD survives. So we are left with the only equation 28. The first Mellin moment is expressed as,

$$B(-t) = \int x dx G_{q,3}(x, 0, -t) \quad (30)$$

$$B(-t) = - \int x dx \tilde{E}_{2T}(x, 0, -t) \quad (31)$$

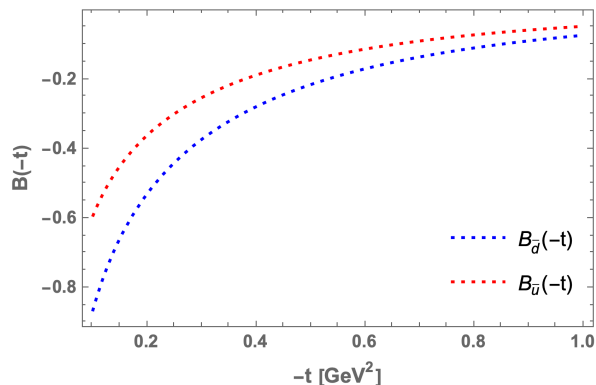


FIG. 4: Gravitational form factor $B(t)$ plotted against energy transfer ‘ $-t$ ’, the red dotted line represents the \bar{u} and the blue dotted line represents the \bar{d} .

Using Ji’s sum rule [6], which relates the total angular momentum with GPDs, we can investigate the twist-3 contribution of sea quarks to the total angular momentum. From figure 4, we have observed that with increasing momentum transfer, $B(-t)$ asymptotically approaches zero. So at large momentum transfer the contribution from twist-3 GPDs to orbital angular momentum (OAM) is negligible. At $t \rightarrow 0$, $B^{\bar{u}} = 0.6$ and $B^{\bar{d}} = -0.8$. Hence, at low energy transfer \bar{u} has larger contributions to OAM of proton than \bar{d} .

C. PDF limit

The PDFs are interpreted as parton densities corresponding at a longitudinal momentum fraction x . The PDFs are mathematically defined by quark-quark correlator,

$$\mathcal{F}(x) = \int \frac{dy^-}{2\pi} e^{iy^-x} \langle P, \Lambda | \bar{\psi} \left(-\frac{y}{2} \right) \Gamma \psi \left(\frac{y}{2} \right) | P, \Lambda \rangle \quad (32)$$

In this work, we focus solely on twist-3 chiral-even GPDs. Therefore, we consider the structures $\Gamma = \gamma^i$ and $\gamma^i \gamma_5$. In the forward limit and at zero skewness, there is only one chiral-even GPD that has a PDF structure. This is given by:

$$\int \frac{dy^-}{2\pi} e^{iy^-x} \langle P, \Lambda | \bar{\psi} \left(-\frac{y}{2} \right) \gamma^i \gamma_5 \psi \left(\frac{y}{2} \right) | P, \Lambda \rangle = 2g_T(x) \quad (33)$$

and g_T is connected to the twist-3 GPD H'_{2T} . The expression that connects the two is given by,

$$g_T(x) = \lim_{\Delta \rightarrow 0} H'_{2T}(x, 0, -t) \quad (34)$$

Equations 23 and 34 show that g_T measures the transverse spin distribution for quarks. It’s very hard to experimentally measure the value of g_T . In this work we have calculated the theoretical values for g_T and also plotted the evolution of g_T with respect to x at different values of transverse momentum transfer ‘ Δ_T^2 ’, in figure 5.

Our key observation is that the g_T as a function of x decreases as the value of x increases. For larger values of Δ_T^2 , PDF becomes negligible, and the magnitude of $g_T^{\bar{u}}$ is larger than $g_T^{\bar{d}}$. Although g_T doesn’t have direct partonic probability interpretation, it is sensitive to the quark-gluon correlation [55]. The Burkhardt-Cottingham sum rule [53] relates the twist-3 PDF $g_T(x)$ and twist-2 PDF $g_1(x)$. The expression of the sum rule is,

$$\int_{-1}^1 g_2(x) dx = 0; \quad \text{where } g_2(x) = g_T(x) - g_1(x) \quad (35)$$

Validation of this sum rule implies that the contributions of quark spin to the proton spin, under different polarization states, are identical. We have numerically checked the sum rule. But in our model, we have observed that both \bar{u} and \bar{d} violate the sum rule because of the presence of the quark mass terms [56]. This violation also indicates the breaking of rotational invariance in our model.

V. CONCLUSION

In this paper, we investigate the twist-3 chiral-even generalized parton distributions (GPDs) of light sea

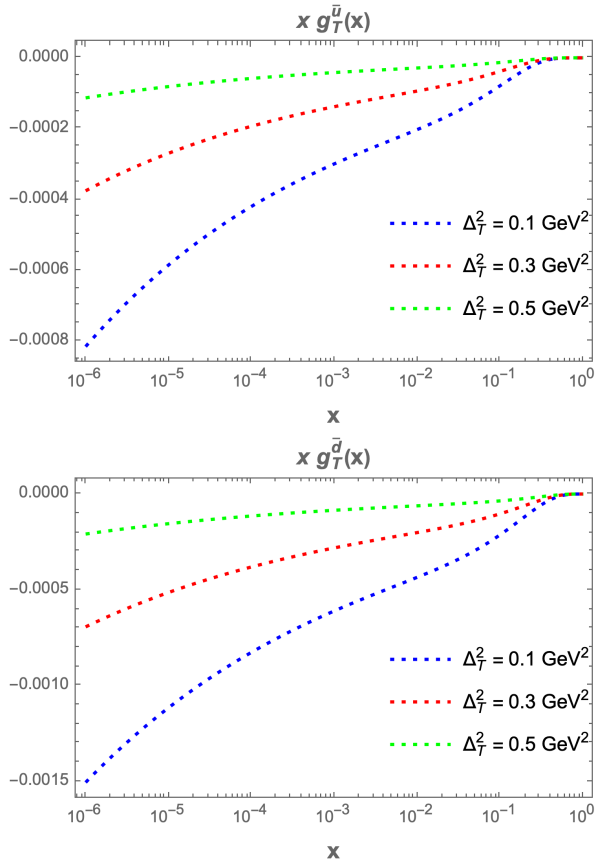


FIG. 5: Twist-3 PDF $xg_T(x)$ is plotted against x at different energy transfers Δ_T^2 ; the top plot is for \bar{u} and the bottom plot is for \bar{d} .

quarks, specifically \bar{u} and \bar{d} , within the light-front spectator model framework. Utilizing the parameterizations outlined in [21, 47], we express the GPDs through light-front wave functions. Our formalism closely follows the basis light-front quantization (BLFQ) approach presented in [45]. We provide a comprehensive analysis of two-dimensional (2D) and three-dimensional (3D) representations of the GPDs to illustrate their behavior across various values of transverse momentum transfer, Δ_T^2 , and longitudinal momentum fraction, x . Additionally, we explore higher-order Mellin moments and, by applying different GPD parameterizations, investigate the gravitational form factor $B(t)$ for \bar{u} and \bar{d} quarks. Lastly, we examine the twist-3 parton distribution function (PDF) g_T for the sea quarks.

The investigation of higher-twist generalized parton distributions (GPDs) of sea quarks is less explored compared to the extensive research on leading-twist GPDs. In future studies, we intend to compute higher-twist GPDs for sea quarks at non-zero skewness ($\xi \neq 0$), accounting for contributions from higher Fock states. The study of non-zero skewness is particularly pertinent to the twist-3 cross-section of deeply virtual Compton scattering (DVCS) [37], which will be examined in upcom-

ing experiments at the Electron-Ion Collider (EIC) and the Electron-Ion Collider in China (EicC) [57]. This research will also enable us to investigate the relationships between higher-twist GPDs and orbital angular momentum distributions. Understanding higher-twist effects will yield qualitative insights into the internal structure of the proton and contribute to addressing longstanding questions, such as the proton spin puzzle and the proton mass problem.

Appendix A

The parametrization of the quark-quark correlator is given in equations 3 and 4. According to the initial and final helicity of the particle, we can reduce these equations. For $j = 1$, we have

$$\begin{aligned} F_{[++] }^{\gamma 1} &= \frac{\Delta^1}{2P^+} (E_{2T} + 2\tilde{H}_{2T}) + \frac{i\Delta^2}{2P^+} (\tilde{E}_{2T} - \xi E_{2T}) \\ F_{[--] }^{\gamma 1} &= \frac{\Delta^1}{2P^+} (E_{2T} + 2\tilde{H}_{2T}) - \frac{i\Delta^2}{2P^+} (\tilde{E}_{2T} - \xi E_{2T}) \end{aligned} \quad (\text{A1})$$

$$\begin{aligned} F_{[++] }^{\gamma 1 \gamma 5} &= \frac{i\Delta^2}{2P^+} (E'_{2T} + 2\tilde{H}'_{2T}) - \frac{\Delta^1}{2P^+} (\tilde{E}'_{2T} - \xi E'_{2T}) \\ F_{[--] }^{\gamma 1 \gamma 5} &= \frac{i\Delta^2}{2P^+} (E'_{2T} + 2\tilde{H}'_{2T}) + \frac{\Delta^1}{2P^+} (\tilde{E}'_{2T} - \xi E'_{2T}) \end{aligned} \quad (\text{A2})$$

$$\begin{aligned} F_{[+-] }^{\gamma 1} &= -\frac{M}{P^+} H_{2T} - \frac{(\Delta^1 + i\Delta^2)\Delta^1}{2MP^+} \tilde{H}_{2T} \\ F_{[-+] }^{\gamma 1} &= \frac{M}{P^+} H_{2T} - \frac{(-\Delta^1 + i\Delta^2)\Delta^1}{2MP^+} \tilde{H}_{2T} \end{aligned} \quad (\text{A3})$$

$$\begin{aligned} F_{[+-] }^{\gamma 1 \gamma 5} &= \frac{M}{P^+} H'_{2T} - \frac{i(\Delta^1 + i\Delta^2)\Delta^2}{2MP^+} \tilde{H}'_{2T} \\ F_{[-+] }^{\gamma 1 \gamma 5} &= -\frac{M}{P^+} H'_{2T} - \frac{i(-\Delta^1 + i\Delta^2)\Delta^2}{2MP^+} \tilde{H}'_{2T} \end{aligned} \quad (\text{A4})$$

Similarly for $j = 2$ we have the following,

$$\begin{aligned} F_{[++] }^{\gamma 2} &= \frac{\Delta^2}{2P^+} (E_{2T} + 2\tilde{H}_{2T}) - \frac{i\Delta^1}{2P^+} (\tilde{E}_{2T} - \xi E_{2T}) \\ F_{[--] }^{\gamma 2} &= \frac{\Delta^2}{2P^+} (E_{2T} + 2\tilde{H}_{2T}) + \frac{i\Delta^1}{2P^+} (\tilde{E}_{2T} - \xi E_{2T}) \end{aligned} \quad (\text{A5})$$

$$\begin{aligned} F_{[++] }^{\gamma 2 \gamma 5} &= -\frac{i\Delta^1}{2P^+} (E'_{2T} + 2\tilde{H}'_{2T}) - \frac{\Delta^2}{2P^+} (\tilde{E}'_{2T} - \xi E'_{2T}) \\ F_{[--] }^{\gamma 2 \gamma 5} &= -\frac{i\Delta^1}{2P^+} (E'_{2T} + 2\tilde{H}'_{2T}) + \frac{\Delta^2}{2P^+} (\tilde{E}'_{2T} - \xi E'_{2T}) \end{aligned} \quad (\text{A6})$$

$$\begin{aligned}
F_{[+-]}^{\gamma^2} &= -\frac{iM}{P^+} H_{2T} - \frac{(\Delta^1 + i\Delta^2)\Delta^2}{2MP^+} \tilde{H}_{2T} \\
F_{[-+]}^{\gamma^2} &= -\frac{iM}{P^+} H_{2T} - \frac{(-\Delta^1 + i\Delta^2)\Delta^2}{2MP^+} \tilde{H}_{2T} \quad (A7)
\end{aligned}$$

$$\begin{aligned}
F_{[+-]}^{\gamma^2\gamma_5} &= \frac{iM}{P^+} H'_{2T} - \frac{i(\Delta^1 + i\Delta^2)\Delta^1}{2MP^+} \tilde{H}'_{2T} \\
F_{[-+]}^{\gamma^2\gamma_5} &= -\frac{iM}{P^+} H'_{2T} - \frac{i(-\Delta^1 + i\Delta^2)\Delta^1}{2MP^+} \tilde{H}'_{2T} \quad (A8)
\end{aligned}$$

Appendix B

Some standard Gaussian integrals that are used in our calculations are,

$$\begin{aligned}
F &= \int_0^\infty k^n dk \text{Exp}[-ak^2] \\
&= \frac{\sqrt{\pi}}{2\sqrt{a}} \quad \text{For } n = 0 \text{ and } \text{Re}[a] > 0 \quad (B1)
\end{aligned}$$

$$= \frac{1}{2a} \quad \text{For } n = 1 \text{ and } \text{Re}[a] > 0 \quad (B2)$$

$$= \frac{\sqrt{\pi}}{4a^{3/2}} \quad \text{For } n = 2 \text{ and } \text{Re}[a] > 0 \quad (B3)$$

$$= \frac{1}{2a^2} \quad \text{For } n = 3 \text{ and } \text{Re}[a] > 0 \quad (B4)$$

-
- [1] A. Deur, S. J. Brodsky, and G. F. De Téramond, The spin structure of the nucleon, Reports on Progress in Physics **82**, 076201 (2019).
- [2] S. Boffi and B. Pasquini, Generalized parton distributions and the structure of the nucleon, La Rivista del Nuovo Cimento **30**, 387 (2007).
- [3] S. Kuhn, J.-P. Chen, and E. Leader, Spin structure of the nucleon—status and recent results, Progress in Particle and Nuclear Physics **63**, 1 (2009).
- [4] B. Filippone and X. Ji, The spin structure of the nucleon, in *Advances in nuclear physics* (Springer, 2001) pp. 1–88.
- [5] C. A. Aidala, S. D. Bass, D. Hasch, and G. K. Mallot, The spin structure of the nucleon, Reviews of Modern Physics **85**, 655 (2013).
- [6] X. Ji, Gauge-invariant decomposition of nucleon spin, Physical Review Letters **78**, 610 (1997).
- [7] X. Ji, Deeply virtual compton scattering, Physical Review D **55**, 7114 (1997).
- [8] A. Radyushkin, Scaling limit of deeply virtual compton scattering, Physics Letters B **380**, 417 (1996).
- [9] A. V. Belitsky, D. Mueller, and A. Kirchner, Theory of deeply virtual compton scattering on the nucleon, Nuclear Physics B **629**, 323 (2002).
- [10] H. Hashamipour, M. Goharipour, and S. S. Gousheh, Determination of generalized parton distributions through a simultaneous analysis of axial form factor and wide-angle Compton scattering data, Phys. Rev. D **102**, 096014 (2020), arXiv:2006.05760 [hep-ph].
- [11] S. Goloskokov and P. Kroll, The longitudinal cross section of vector meson electroproduction, The European Physical Journal C **50**, 829 (2007).
- [12] S. Goloskokov and P. Kroll, The role of the quark and gluon gpdfs in hard vector-meson electroproduction, The European Physical Journal C **53**, 367 (2008).
- [13] S. V. Goloskokov and P. Kroll, An attempt to understand exclusive π^+ electroproduction, The European Physical Journal C **65**, 137 (2010).
- [14] S. Goloskokov and P. Kroll, Transversity in hard exclusive electroproduction of pseudoscalar mesons, The European Physical Journal A **47**, 112 (2011).
- [15] C. Adloff, V. Andreev, B. Andrieu, T. Anthonis, A. Astvatsatourov, A. Babaev, J. Bähr, P. Baranov, E. Barrelet, W. Bartel, *et al.*, Diffractive photoproduction of ψ (2s) mesons at hera, Physics Letters B **541**, 251 (2002).
- [16] F. D. Aaron, M. A. Martin, C. Alexa, K. Alimujiang, V. Andreev, B. Antunovic, S. Backovic, A. Baghdasaryan, E. Barrelet, W. Bartel, *et al.*, Deeply virtual compton scattering and its beam charge asymmetry in $e\pm p$ collisions at hera, Physics Letters B **681**, 391 (2009).
- [17] Z. Collaboration *et al.*, A measurement of the q^2 , w and t dependences of deeply virtual compton scattering at hera, Journal of High Energy Physics **2009**, 108 (2009).
- [18] A. Airapetian, N. Akopov, Z. Akopov, E. Aschenauer, W. Augustyniak, R. Avakian, A. Avetissian, E. Avetisyan, H. Blok, A. Borisso, *et al.*, Beam-helicity and beam-charge asymmetries associated with deeply virtual compton scattering on the unpolarised proton, Journal of High Energy Physics **2012** (2012).
- [19] A. Airapetian, N. Akopov, Z. Akopov, E. Aschenauer, W. Augustyniak, R. Avakian, A. Avetissian, E. Avetisyan, S. Belostotski, H. Blok, *et al.*, Beam-helicity asymmetry arising from deeply virtual compton scattering measured with kinematically complete event reconstruction, Journal of High Energy Physics **2012**, 1 (2012).
- [20] N. d'Hose, E. Burtin, P. Guichon, and J. Marroncle, Feasibility study of deeply virtual compton scattering using compass at cern, in *Perspectives in Hadronic Physics: 4th International Conference Held at ICTP, Trieste, Italy, 12–16 May 2003* (Springer, 2004) pp. 47–53.
- [21] S. Stepanyan, V. Burkert, L. Elouadrhiri, G. Adams, E. Anciant, M. Anghinolfi, B. Asavapibhop, G. Audit, T. Auger, H. Avakian, *et al.*, Observation of exclusive deeply virtual compton scattering in polarized electron beam asymmetry measurements, Physical Review Letters **87**, 182002 (2001).
- [22] M. Goharipour, H. Hashamipour, F. Irani, and K. Azizi (MMGPDs), Impact of JLab data on the determination of GPDs at zero skewness and new insights from transition form factors $N \rightarrow \Delta$, Phys. Rev. D **109**, 074042 (2024), arXiv:2403.19384 [hep-ph].
- [23] X. Ji, W. Melnitchouk, and X. Song, Study of off-forward parton distributions, Physical Review D **56**, 5511 (1997).

- [24] S. Scopetta and V. Vento, Generalized parton distributions and composite constituent quarks, *Physical Review D* **69**, 094004 (2004).
- [25] H.-M. Choi, C.-R. Ji, and L. Kisslinger, Continuity of generalized parton distributions for the pion virtual compton scattering, *Physical Review D* **66**, 053011 (2002).
- [26] H.-M. Choi, C.-R. Ji, and L. Kisslinger, Skewed quark distribution of the pion in the light-front quark model, *Physical Review D* **64**, 093006 (2001).
- [27] H. Mineo, S. N. Yang, C.-Y. Cheung, and W. Bentz, Generalized parton distributions of the nucleon in the nambu-jona-lasinio model based on the faddeev approach, *Physical Review C—Nuclear Physics* **72**, 025202 (2005).
- [28] K. Goeke, V. Guzey, and M. Siddikov, Generalized parton distributions and deeply virtual compton scattering in color glass condensate model, *The European Physical Journal C* **56**, 203 (2008).
- [29] K. Goeke, M. V. Polyakov, and M. Vanderhaeghen, Hard exclusive reactions and the structure of hadrons, *Progress in Particle and Nuclear Physics* **47**, 401 (2001).
- [30] J. Ossmann, M. Polyakov, P. Schweitzer, D. Urbano, and K. Goeke, Generalized parton distribution function ($e^+e^- \rightarrow e^+e^- \gamma$) of the nucleon in the chiral quark soliton model, *Physical Review D—Particles, Fields, Gravitation, and Cosmology* **71**, 034011 (2005).
- [31] B. Tiburzi and G. Miller, Exploring skewed parton distributions with two-body models on the light front. ii. covariant bethe-salpeter approach, *Physical Review D* **65**, 074009 (2002).
- [32] S. Noguera, L. Theußl, and V. Vento, Generalized parton distributions of the pion in a bethe-salpeter approach, *The European Physical Journal A—Hadrons and Nuclei* **20**, 483 (2004).
- [33] B. Pasquini and S. Boffi, Virtual meson cloud of the nucleon and generalized parton distributions, *Physical Review D—Particles, Fields, Gravitation, and Cosmology* **73**, 094001 (2006).
- [34] B. Pasquini and S. Boffi, Generalized parton distributions in a meson cloud model, *Nuclear Physics A* **782**, 86 (2007).
- [35] R. Jaffe and A. Manohar, The g_1 problem: Deep inelastic electron scattering and the spin of the proton, *Nuclear Physics B* **337**, 509 (1990).
- [36] Y. Hatta and S. Yoshida, Twist analysis of the nucleon spin in qcd, *Journal of high energy physics* **2012**, 1 (2012).
- [37] Y. Guo, X. Ji, B. Kriesten, and K. Shiells, Twist-three cross-sections in deeply virtual compton scattering, *Journal of High Energy Physics* **2022**, 1 (2022).
- [38] M. Burkardt, Transverse force on quarks in deep-inelastic scattering, *Physical Review D—Particles, Fields, Gravitation, and Cosmology* **88**, 114502 (2013).
- [39] F. P. Aslan, M. Burkardt, and M. Schlegel, Transverse force tomography, *Physical Review D* **100**, 096021 (2019).
- [40] A. Mukherjee and M. Vanderhaeghen, Off-forward matrix elements in light-front hamiltonian qcd, *Physics Letters B* **542**, 245 (2002).
- [41] A. Mukherjee and M. Vanderhaeghen, Helicity-dependent twist-two and twist-three generalized parton distributions in light-front qcd, *Physical Review D* **67**, 085020 (2003).
- [42] F. P. Aslan and M. Burkardt, Singularities in twist-3 quark distributions, *Physical Review D* **101**, 016010 (2020).
- [43] S. Sharma and H. Dahiya, Twist-4 proton gtdms in the light-front quark-diquark model, *The European Physical Journal A* **59**, 235 (2023).
- [44] S. Bhattacharya, K. Cichy, M. Constantinou, J. Dodson, A. Metz, A. Scapellato, and F. Steffens, Chiral-even axial twist-3 gtdms of the proton from lattice qcd, *Physical Review D* **108**, 054501 (2023).
- [45] Z. Zhang, Z. Hu, S. Xu, C. Mondal, X. Zhao, J. P. Vary, and B. Collaboration, Twist-3 generalized parton distribution for the proton from basis light-front quantization, *Physical Review D* **109**, 034031 (2024).
- [46] S. Meißner, A. Metz, and M. Schlegel, Generalized parton correlation functions for a spin-1/2 hadron, *Journal of High Energy Physics* **2009**, 056 (2009).
- [47] A. Rajan, M. Engelhardt, and S. Liuti, Lorentz invariance and qcd equation of motion relations for generalized parton distributions and the dynamical origin of proton orbital angular momentum, *Physical Review D* **98**, 074022 (2018).
- [48] S. J. Brodsky, D. S. Hwang, B.-Q. Ma, and I. Schmidt, Light-cone representation of the spin and orbital angular momentum of relativistic composite systems, *Nuclear Physics B* **593**, 311 (2001).
- [49] P. Choudhary, D. Chakrabarti, and C. Mondal, Flavor asymmetry of light sea quarks in proton: a light-front spectator model, *Eur. Phys. J. C* **84**, 626 (2024), arXiv:2312.01484 [hep-ph].
- [50] D. Chakrabarti and C. Mondal, Generalized parton distributions for the proton in ads/qcd, *Physical Review D—Particles, Fields, Gravitation, and Cosmology* **88**, 073006 (2013).
- [51] S. J. Brodsky, H.-C. Pauli, and S. S. Pinsky, Quantum chromodynamics and other field theories on the light cone, *Physics Reports* **301**, 299 (1998).
- [52] A. Harindranath, An introduction to light-front dynamics for pedestrians, arXiv preprint hep-ph/9612244 (1996).
- [53] H. Burkhardt and W. Cottingham, Sum rules for forward virtual compton scattering, *Annals of Physics* **56**, 453 (1970).
- [54] Y. Guo, X. Ji, and K. Shiells, Novel twist-three transverse-spin sum rule for the proton and related generalized parton distributions, *Nuclear Physics B* **969**, 115440 (2021).
- [55] R. L. Jaffe and X. Ji, Chiral-odd parton distributions and drell-yan processes, *Nuclear Physics B* **375**, 527 (1992).
- [56] S. Bhattacharya and A. Metz, Burkhardt-cottingham-type sum rules for light-cone and quasi-pdfs, *Physical Review D* **105**, 054027 (2022).
- [57] M. Diehl, Generalized parton distributions with helicity flip, *The European Physical Journal C—Particles and Fields* **19**, 485 (2001).
- [58] S. Boffi, B. Pasquini, and M. Traini, Linking generalized parton distributions to constituent quark models, *Nuclear Physics B* **649**, 243 (2003).

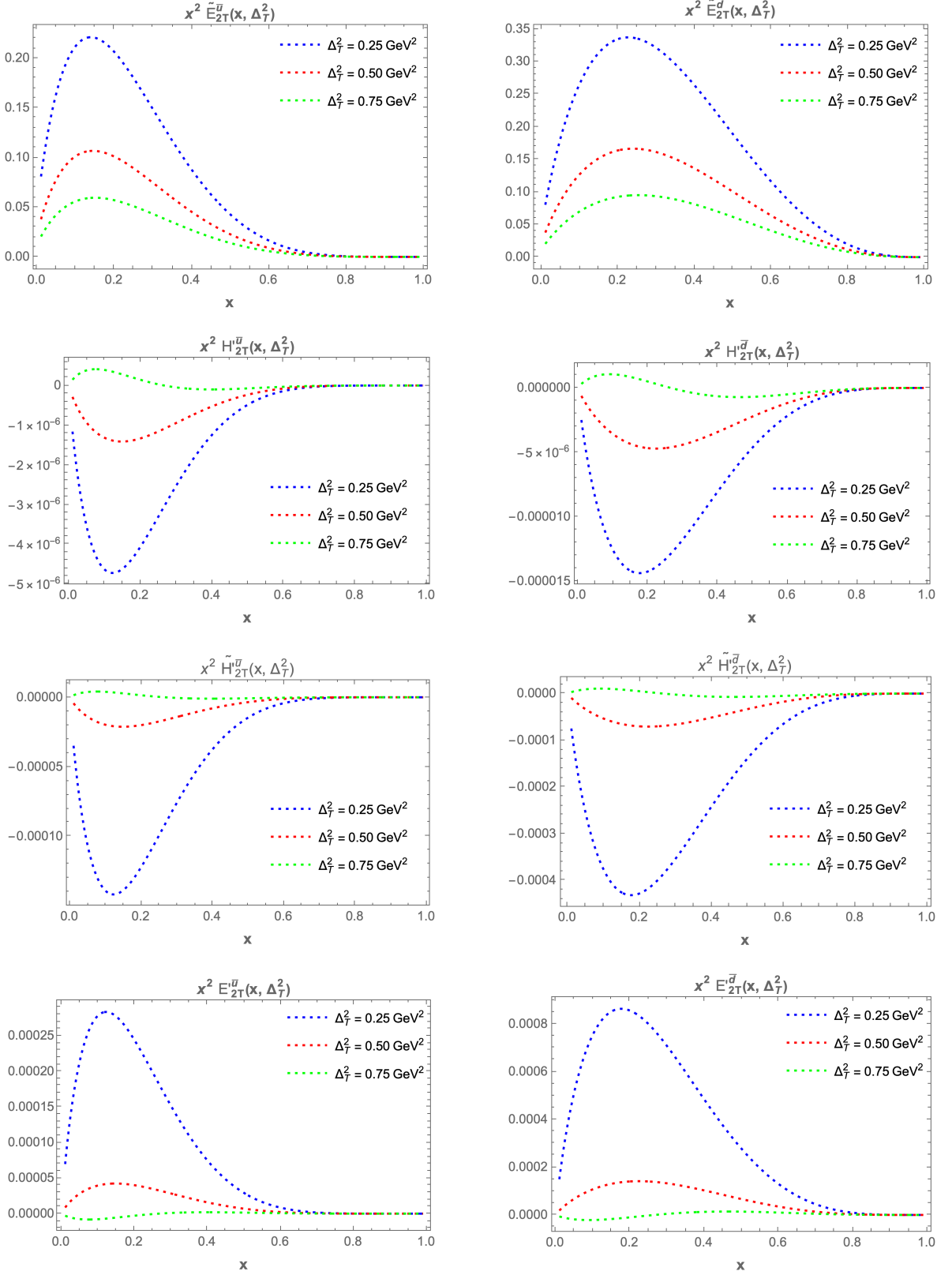


FIG. 6: The Twist-3 chiral even GPDs $x^2 \tilde{E}_{2T}$, $x^2 \tilde{H}'_{2T}$, $x^2 E'_{2T}$, and $x^2 H_{2T}$ are plotted as functions of x for fixed values of $\Delta_T^2 = 0.25 \text{ GeV}^2$ (blue), 0.50 GeV^2 (red), and 0.75 GeV^2 (green). The left column of the plots corresponds to the distributions for \bar{u} , while the right column corresponds to \bar{d} .

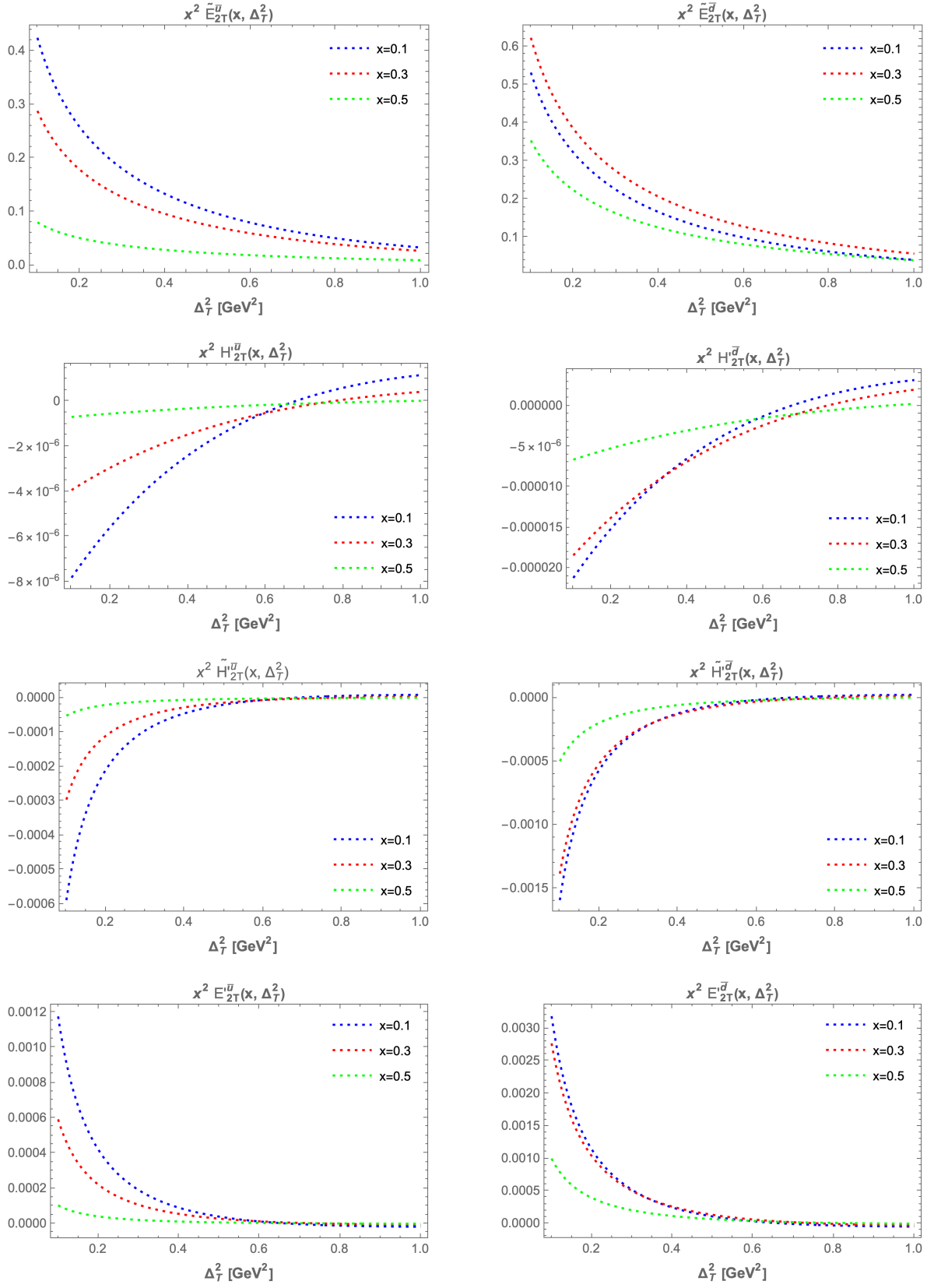


FIG. 7: The Twist-3 chiral even GPDs $x^2 \bar{E}_{2T}$, $x^2 \bar{H}'_{2T}$, $x^2 E'_{2T}$, and $x^2 H'_{2T}$ are plotted as functions of Δ_T^2 for fixed values of $x = 0.1$ (blue), 0.3 (red), and 0.5 (green). The left column of the plots corresponds to the distributions for \bar{u} , while the right column corresponds to \bar{d} .